Article:

Proofs to Dr. M.A. Halcrow,

School of Chemistry, University of Leeds, Woodhouse Lane, Leeds LS2 9JT, UK.

Spin State Behaviour of Iron(II)/Dipyrazolylpyridine Complexes. New Insights from Crystallographic and Solution Measurements

Laurence J. Kershaw Cook[a], Rufeida Mohammed[a], Grant Sherborne[a], Thomas D. Roberts[a], Santiago Alvarez[b,*] and Malcolm A. Halcrow[a,*]

[a]*School of Chemistry, University of Leeds, Woodhouse Lane, Leeds LS2 9JT, U.K.*

Fax: (+44) 113 343 6565.   Email: M.A.Halcrow@leeds.ac.uk.

[b]*Departament de Química Inorgànica and Institut de Química Teòrica i Computacional,*

Universitat de Barcelona, Marti i Franquès 1-11,

08028 Barcelona, Spain

Email: santiago.alvarez@qi.ub.es

Abstract

Abstract

The isomeric complexes $[Fe(1\text{-}bpp)_2]^{2+}$ and $[Fe(3\text{-}bpp)_2]^{2+}$ (1-bpp = 2,6-di[pyrazol-1-yl]pyridine; 3-bpp = 2,6-di[1*H*-pyrazol-3-yl]pyridine) and their derivatives are some of the most widely investigated complexes in spin-crossover research. This article addresses two unique aspects of their spin-state chemistry. First, is an unusual structural distortion in the high-spin form that can inhibit spin-crossover in the solid state. A new analysis of these structures using continuous shape measures has explained this distortion in terms of its effect on the metal coordination geometry, and has shown that the most highly distorted structures are a consequence of crystal packing effects. Second, solution studies have quantified the influence of second-sphere hydrogen bonding on spin-crossover in $[Fe(3\text{-}bpp)_2]^{2+}$, which responds to the presence of different anions and solvents (especially water). Previously unpublished data from the unsymmetric isomer $[Fe(1,3\text{-}bpp)_2]^{2+}$ (1,3-bpp = 2-[pyrazol-1-yl]-6-[1*H*-pyrazol-3-yl]pyridine) are presented for comparison. Modifications to the structure of $[Fe(3\text{-}bpp)_2]^{2+}$, intended to augment these supramolecular effects, are also described.

Highlights:

- High-spin $[Fe(1\text{-}bpp)_2]^{2+}$ derivatives often adopt highly distorted six-coordinate geometries in the crystal, that can strongly affect their spin-state properties.

- This corresponds to a Bailar twist distortion, modified by the narrow ligand bite angle. The most distorted stereochemistries are imposed by crystal packing effects.

- The solution phase spin-equilibrium in $[Fe(3\text{-}bpp)_2]^{2+}$ is unusually sensitive to changes to the solvent and anions, and is particularly responsive to water.

- Addition of hydrogen bonding or hydrophobic pyrazole substituents onto $[Fe(3\text{-}bpp)_2]^{2+}$ stabilizes its high-spin state.

1.   Introduction

The complexes $[Fe(1\text{-}bpp)_2]^{2+}$ and $[Fe(3\text{-}bpp)_2]^{2+}$ (1-bpp = 2,6-di[pyrazol-1-yl]pyridine; 3-bpp = 2,6-di[1H-pyrazol-3-yl]pyridine; Scheme 1), and their derivatives [1-3], are both widely used in spin-crossover research [4-7]. Their popularity reflects different and complementary aspects of their chemistry. On one hand, synthetic methods are available to derivatise the 1-bpp ligand at every position of the ligand skeleton [1], allowing a wide variety of substituted $[Fe(1\text{-}bpp)_2]^{2+}$ derivatives to be prepared. Substituents at the pyrazolyl $C3$ positions have a strong influence on the spin-state of the iron center, on steric and electronic grounds [8]. Conversely, substituents at the pyridyl $C4$ sites have no steric impact on the metal ion, which allows functional substituents to be appended to the $[Fe(1\text{-}bpp)_2]^{2+}$ center while retaining spin-crossover activity. Thus, multifunctional derivatives of $[Fe(1\text{-}bpp)_2]^{2+}$ bearing peripheral metal-binding domains [9] or conducting [10], fluorescent [11], photoswitchable [12], radical [13], redox active [10, 14] and surface tether substituents [15] have all been reported. None of the other commonly used spin-crossover centers affords this degree of variety in its synthetic chemistry.

<Insert Scheme 1 here>

The synthetic chemistry of 3-bpp is less well developed, although some $[Fe(3\text{-}bpp)_2]^{2+}$ derivatives bearing substituents at the pyrazolyl $N1$ and $C5$ positions have recently been reported [3, 16-19]. Rather, the unique properties of $[Fe(3\text{-}bpp)_2]^{2+}$ stem from its hydrogen-bonding capabilities. The complex has Lewis acidic $N-H$ groups adjacent to four of its six metal donor N atoms, and changes to the hydrogen bonding of these groups are efficiently transmitted to the iron center and have a strong impact on its spin state. This makes solid salts of $[Fe(3\text{-}bpp)_2]^{2+}$ particularly sensitive to the anions and solvent present in the material, especially to the degree of hydration. Moreover, $[Fe(3\text{-}bpp)_2]^{2+}$ can be recrystallised from

water, which makes it easy to precipitate salts of that complex with different anions. Thus, more salts of $[Fe(3\text{-}bpp)_2]^{2+}$ have been investigated for their spin-state properties than for any other cationic complex [1, 3]. Both these aspects may contribute to the high incidence of cooperative spin-crossover and novel structural chemistry in salts of $[Fe(3\text{-}bpp)_2]^{2+}$ and its derivatives [17-20]. The aqueous stability of $[Fe(3\text{-}bpp)_2]^{2+}$ is unusual, and contrasts with $[Fe(1\text{-}bpp)_2]^{2+}$ which hydrolyses spontaneously in water. This question is addressed below.

Despite these advantages, both classes of complex also have a significant drawback for spin-crossover research, which is that their high-spin complexes are prone to adopt an unusual angular structural distortion in the solid state [2, 3]. The distortion is characterized by two structural components (Scheme 2): a decrease in the *trans*-N−Fe−N angle (ϕ) from its ideal value of 180°; and, a twisting of the two tridentate ligands from the perpendicular, so the dihedral angle between them (θ) is < 90°. The ϕ and θ distortions occur independently of each other in different compounds, and can adopt values in the range $149 \le \phi \le 180°$ and $59 \le \theta \le 90°$ (Figs. 1 and 2). This type of geometry is exhibited by a number of complexes of high-spin d^5 and d^6 ions with meridional *tris*-imine ligands, like 2,2':6',2''-terpyridine [21]. However, it is particularly common in the $[Fe(1\text{-}bpp)_2]^{2+}$ system [11, 12, 22-26], while some examples of $[Fe(3\text{-}bpp)_2]^{2+}$ derivatives exhibiting the distortion have also been published [16, 27]. A DF calculation identified the Jahn-Teller effect as the origin of the distortion, and noted it is favored by a narrow intra-ligand bite angle [22]. That explains its prevalence in $[Fe(1\text{-}bpp)_2]^{2+}$ chemistry, because the intra-ligand *cis*-N−Fe−N angle in a high-spin $[Fe(1\text{-}bpp)_2]^{2+}$ or $[Fe(3\text{-}bpp)_2]^{2+}$ complex is typically 72-73°.

<Insert Scheme 2 and Figs. 1 and 2 here>

Since the Jahn-Teller distortion is only a property of the orbitally degenerate high-spin state, distorted complexes must rearrange to an undistorted low-spin structure if they are to undergo spin-crossover. If the distorted→undistorted rearrangement is too large for a rigid solid lattice to accommodate, the compound remains trapped in its high-spin state at all temperatures [7]. This has led a number of complexes, that might otherwise be expected to be spin-crossover active, to lose their functionality in the solid state. A survey of $[Fe(1\text{-}bpp)_2]^{2+}$ complexes five years ago concluded that high-spin compounds with $\phi < 172°$ and/or $\theta < 76°$ should not exhibit spin-crossover on cooling [2]. A small number of outliers have been discovered since then, which are spin-crossover active despite having more distorted high-spin structures (Fig. 2) [26]. Notably most of these are abrupt, hysteretic spin transitions which may reflect the distorted→undistorted structure changes involved. Be that as it may, it is still the case that the great majority of Jahn-Teller distorted $[Fe(bpp)_2]^{2+}$ complexes do not exhibit spin-crossover (Fig. 2). Importantly, complexes that are distorted in the solid state can still undergo spin-crossover in solution, probably because of rapid interconversion between distorted and undistorted geometries in their labile high-spin states.

This article addresses two questions relevant to $[Fe(1\text{-}bpp)_2]^{2+}$ and $[Fe(3\text{-}bpp)_2]^{2+}$ in spin-crossover research. First, is a new analysis of the Jahn-Teller distortion in $[Fe(1\text{-}bpp)_2]^{2+}$ complexes using shape measure indices, that quantifies the relationship between the distortion and the coordination geometry of the iron(II) ions. Second, is a description of recent work that addresses the unique supramolecular chemistry of $[Fe(3\text{-}bpp)_2]^{2+}$ centres through solution phase measurements. As part of this discussion, the solution and solid state properties of the unsymmetric isomer $[Fe(1,3\text{-}bpp)_2]^{2+}$ (1,3-bpp = 2-[pyrazol-1-yl]-6-[1*H*-pyrazol-3-yl]pyridine; Scheme 1) are also described for the first time.

2.   Stereochemistry of the Jahn Teller Distortion in $[Fe(1\text{-bpp})_2]^{2+}$ Derivatives

Since we first reported it in 2002 [22], we (and others) have quantified the Jahn-Teller distortion in crystalline, high-spin $[Fe(1\text{-bpp})_2]^{2+}$ complexes using indices describing the disposition of the tridentate ligands in the molecule (Scheme 2) [2]. These parameters (ϕ and θ) are relevant to the spin-state properties of the compounds, which are strongly affected by the shape of the complex molecules and their nearest neighbor interactions in the crystal lattice [7]. However we present here a new structural analysis of the distortion, and the structural changes that occur during spin-crossover, in terms of its effect on the metal ion coordination geometry. Since the coordination geometry is an important factor determining ϕ and θ, and thus the overall shape of the molecule, this discussion provides new insight into the variable and unpredictable spin-state behavior of $[Fe(1\text{-bpp})_2]^{2+}$ complexes.

2.1   Introduction to Shape Measures

We have applied the Continuous Shape Measures methodology [28-30] using the *SHAPE 2.1* program [31] to analyse stereochemical trends associated with spin-crossover transitions, and to address structural variations presented by compounds of this family in their high-spin or low-spin states [32]. A shape measure of a set of atoms, such as a metal ion and its first coordination sphere, is the size-weighted sum of the squares of the distances between each atom and the corresponding vertex of the relevant ideal polyhedron [29]. This sum is minimized with respect to translations, rotations and a change of scale of one set of points (*e.g.* the atomic coordinates), and with respect to all possible pairings of the two sets of coordinates. By definition, a zero value of a shape measure indicates a coordination sphere exactly coincident with the reference polyhedron, and non-zero values provide a quantitative

calibration of how much that structure deviates from the reference polyhedron [29]. The symbols S(OC-6) and S(TPR-6) will designate the shape measures of the FeN_6 coordination sphere relative to the octahedron and the trigonal prism, respectively, in the following discussion.

This technique is often useful for analyzing a particular structure by calculating its shape measures relative to two different reference polyhedra, conveniently plotted in a "shape map" [33, 34]. This visualizes whether that structure lies along the minimal distortion path for the interconversion of the two polyhedra. For six-coordinate metal ions, the minimal distortion pathway between the octahedron and the trigonal prism is usually considered [34], which corresponds to the Bailar trigonal twist [35]. A quantitative evaluation of how close (or how far) the structure is from the minimal distortion path is provided by the path deviation function, quoted as a percentage of the deviation relative to the total length of the path [33, 36].

2.2   Analysis of Crystallographic Data

The following analysis concerns the coordination spheres of iron atoms in their low-spin and high-spin states, regardless of whether or not they undergo spin crossover; whether a low spin state has been trapped by fast cooling; or a high spin state has been induced at low temperature by irradiation (the LIESST effect [37]). This includes examples of two crystallographically independent iron centers with different spin states in the same crystal. Structures that are not in a pure spin-state at the temperature of measurement, and structures measured within a spin-crossover hysteresis loop, are disregarded in most of the discussion.

High-spin and low-spin complexes in Figs. 3-6 are identified by upward and downward oriented triangles, respectively [38].

An earlier analysis of the effect of spin-crossover on the coordination geometries of transition ions observed that the longer metal−ligand distances of the high spin state induce smaller bite angles of bidentate ligands, which in turn favors a Bailar twist distortion of the octahedron towards a trigonal bipyramidal geometry [32]. $[Fe(1\text{-bpp})_2]^{2+}$ complexes behave as expected in this regard, with a good correlation between the average Fe−N bond length and the ligand bite angle. More specifically, $[Fe(1\text{-bpp})_2]^{2+}$ complexes belong to a family where two tridentate ligands span perpendicular meridional (*mer*) coordination sites of an octahedron. The two equivalent bite angles in each ligand enforce a deviation of the intra-ligand *trans*-N−Fe−N axes from linearity, imposing D_{2d} symmetry *via* a double axial distortion of the octahedron which is calibrated by the clamp angle φ (Scheme 3) [34]. Such a distortion is enhanced in the high spin configuration due to its smaller ligand bite angle, which in turn leads to a reduction in φ (Scheme 3). As expected, a good correlation is also observed between φ and the Fe−N distance, with the low- and high-spin configurations presenting distinct values of the two parameters (Fig. 3). Data points with the lowest values of φ deviate somewhat from the general trend, and are discussed in more detail below.

<Insert Scheme 3 and Fig. 3 here>

Conversion of an octahedral MX_6 unit to a trigonal prism *via* the Bailar twist pathway results in contraction of the *trans*-X−M−X bond angles, from 180º (octahedron) to 135.6º (trigonal prism) [34]. Moreover, the angle between the planes formed by the two sets of *mer*-MX_3 groups changes from 90º in the octahedron to 60º in the trigonal prism. Thus, a Bailar twist distortion should lead to decreased values of ϕ and θ (Scheme 2) for high spin $[Fe(1\text{-bpp})_2]^{2+}$

complexes, as is often observed (Fig. 2). Notably, however, there is no apparent correlation of ϕ or θ, which vary widely in the high-spin state, with the average Fe−N distance and clamp angle φ. This emphasizes that the Jahn-Teller distortion cannot be described purely in terms of the Bailar twist mechanism.

Since a number of geometrical parameters must be considered to compare the spin-states of $[Fe(1\text{-}bpp)_2]^{2+}$ derivatives, that do not all correlate with each other, we analyzed the geometries of their FeN_6 coordination spheres through a shape map that simultaneously reflects changes in all these parameters. The geometric paths for the Bailar twist and the double axial distortion (φ) of the octahedron are represented in Fig. 4, as a shape map relative to the octahedron and the trigonal prism. Plotting the shape measures of the coordination polyhedra of the compounds affords a wider perspective on the stereochemical consequences of spin crossover. The low- and high-spin molecules occupy well-separated regions on the map, the former exhibiting less distorted octahedra and the latter being more distorted due to an increased double axial distortion. Within each group, however, the structures deviate from the double axial pathway in directions that are roughly parallel to the Bailar twist. It is thus clear that the complexes adopt varying degrees of both the Bailar twist and the clamp distortion in both spin states. A histogram of their path deviation functions relative to the Bailar twist demonstrates that the high-spin complexes deviate more than the low-spin ones from that path (Fig. 5), and show a wider spread of values for the deviation index.

<Insert Figs. 4 and 5 here>

The dependence of the octahedral shape measure on the Fe−N bond length and the clamp angle φ are quite similar (Fig. 6). There is again a clear separation of the high-spin and low-spin complexes, although both spin states follow the same trends for Fe−N ≤ 2.15 Å and $\varphi \geq$

146°. However, at larger distances and smaller φ values, more severe distortions of the coordination octahedron result, which are essentially independent of the Fe−N distance and show a strong dependence on φ. Our previous analysis on complexes with ill-defined coordination numbers [39] implies that the largest deviations from the octahedral geometry could be associated with incipient, additional coordination of donor atoms from counterions or neighboring molecules. Therefore, we surveyed all the high-spin structures for contacts from donor atoms (O, N, F, S, I or P) to iron that are up to 0.3 Å longer than the sum of Van der Waals radii (41 independent molecular structures of this type were found). All the molecules whose OC-6 shape measure is larger than expected, based on its Fe−N distances and φ angle, are involved in such short additional Van der Waals contacts (Fig. 6).

<Insert Fig. 6 here>

A shape analysis of the augmented FeN_6X_n coordination spheres in the above compounds shows that most of them are approaching a monocapped or bicapped trigonal prism, for one ($n = 1$) or two ($n = 2$) short contacts respectively. There is a good correlation between the Fe…X contact distance and the shape measure of the iron augmented coordination sphere relative to a capped trigonal prism (Fig. 7). Only five compounds deviate significantly from this trend. Two (isostructural) compounds show an expanded coordination polyhedron closer to a capped octahedron than a capped trigonal prism; in two others the iron atom seems to feel the stabilizing effect of the distortion at somewhat longer Fe…X distances, since the FeN_6 core is relatively close to the trigonal prism ideal; and the fifth one is better described as a snub disphenoid than a capped trigonal prism, which reflects the chelating nature of two contacting O atoms from a neighboring ligand nitro substituent. Inspection of the structures closest to the trigonal prism indicates that full conversion to that polyhedron would lead to

the coordination topology shown in Fig. 8, where each tridentate ligand occupies three vertices of a different square face of the prism.

<Insert Figs. 7 and 8 here>

Although ϕ and θ (Scheme 2) do not correlate with the expansion of the iron coordination sphere, the greatest deviations of these parameters from their ideal octahedral values do also correlate reasonably with the intermolecular Fe$\cdots$X distance. Hence, the largest Bailar distortions and the associated decreases in ϕ and θ are both stabilized by the incipient coordination of extra donor atoms. The correlation between ϕ and Fe$\cdots$X is particularly clear, and has only six outliers. Three of these correspond to larger X atoms (S or I) compared to those following the main trend (X = N, O or F), while the other three are structures presenting two Fe$\cdots$X contacts at about the same distance, thus favoring a larger distortion than the single contact observed in the rest of compounds. These plots are shown in the Supporting Information.

2.3 Summary

To conclude, the distorted coordination geometries observed in high-spin $[Fe(bpp)_2]^{2+}$ complexes are a combination of a typical Bailar twist towards a trigonal prismatic structure (Fig. 8) [34]; and the double axial distortion enforced by the ligand bite angle, which becomes more severe at longer Fe−N bond distances (φ in Scheme 3) [32]. When $\varphi \geq 146º$ there is a regular relationship between φ and the distortion of the coordination geometry away from an ideal octahedron. When φ is smaller, the coordination geometry deviates more strongly towards capped or bicapped trigonal prismatic, depending on the presence or absence of short intermolecular contacts to the iron center (Figs. 6 and 7). The most strongly

13

distorted structures all exhibit such intermolecular contacts, in face-capping positions relative to the inner coordination polyhedron, and their coordination geometry correlates strongly with the length of these contacts (Fig. 8). Hence, while a wide range of Jahn-Teller distortion structures is accessible to high-spin $[Fe(1-bpp)_2]^{2+}$ complexes (Fig. 2), the observation of a specific distortion in a particular compound is a reflection of its crystal packing.

The significant angular distortions of the high-spin $[Fe(1-bpp)_2]^{2+}$ coordination sphere are therefore a geometric consequence of the Fe−N bond elongation, combined with the constraints of the *mer*-tridentate ligand. The ensuing Bailar twist, that converts a triangular face of the octahedron into a square face of a trigonal prism, facilitates the interaction of counterions or solvent molecules with the metal ion, thus stabilizing the highly twisted geometries. Consistent with that conclusion, analogous complexes with monodentate N-heterocyclic ligands are all nearly perfect octahedra [S(OC-6) < 0.44], even in the high spin state, since the Fe−N elongation does not imply an angular distortion of the octahedron in this case [32]. Finally, a preliminary survey of the $[Fe(3-bpp)_2]^{2+}$ family of complexes also gave results consistent with this conclusion, including some examples of extended coordination spheres in the high spin state.

3. Supramolecular Chemistry of $[Fe(3-bpp)_2]^{2+}$ and its Derivatives

3.1   Background

With inspiration from Shores' and Hooley's recent work on spin-transitions in solution triggered by host:guest binding [40, 41], we decided to examine the supramolecular chemistry of $[Fe(3-bpp)_2]^{2+}$ in more depth. The chemistry of $[Fe(3-bpp)_2]^{2+}$ was originally developed by Goodwin *et al.* during the 1990s [1, 42-44], who noted the strong correlation

between the spin states of of solid $[Fe(3\text{-bpp})_2]^{2+}$ salts and the presence of lattice water, which stabilizes the low-spin form of the complex [42, 43, 45]. They also published solution phase magnetic data for three different salts $[Fe(3\text{-bpp})_2]X_2$ ($X^- = BF_4^-$, PF_6^- and I^-), concluding that "all three salts show essentially the same behavior" [43]. However, we noted that the iodide salt undergoes spin-crossover in solution at *ca.* 10 K higher temperature than the other salts, according to their published data. Although the difference is small, that is the trend expected if there is significant $N-H{\ldots}I^-$ hydrogen bonding between the cation and anions in solution [40]. Both these aspects implied that the spin state of $[Fe(3\text{-bpp})_2]^{2+}$ may be very sensitive to changes to its second coordination sphere.

3.2   Solvent Dependence

The easiest way to probe this question was to determine the spin-crossover equilibrium of $[Fe(3\text{-bpp})_2]^{2+}$ in different solvents. Evans method measurements yielded the following trend in $T_{\frac{1}{2}}$ for six deuterated solvents (Fig. 9) [46]:

$$CD_3NO_2\ (T_{\frac{1}{2}} = 244\ K) \approx CD_3CN\ (244) \approx (CD_3)_2CO\ (247) < CD_3OD\ (255) \approx$$

$$(CD_3)_2NCDO\ (257) << D_2O\ (317)$$

That trend correlates with measures of solvent donacity including the Gutman donor number D_N [47] and Kamlet and Taft's β parameter [48], which shows that more strongly donating solvents stabilize the low-spin state of the complex. The solvent-dependence shown by $[Fe(3\text{-bpp})_2]^{2+}$ is stronger than for any other published compound [49, 50], and the 60-70 K increase of $T_{\frac{1}{2}}$ in water compared to the organic solvents is especially striking. For comparison, $[Fe(tacn)_2]^{2+}$ (tacn = 1,4,7-triazacyclononane) which has six hydrogen bond-donor $N-H$ functions in each molecule, exhibits $T_{\frac{1}{2}} = 318$ K in CD_3CN and 343 K in D_2O which is only 25 K higher in water [50].

<Insert Figure 9 here>

Further insight was gained from measurements of $[Fe(3-bpp)_2]^{2+}$ in acetone:water solvent mixtures. These showed that $T_{1/2}$ increases with the mole fraction of water present, as expected. However the relationship was non-linear, with a plateau region at intermediate solvent compositions where $T_{1/2}$ was almost independent of the water content [46]. The measured enthalpy of spin-crossover also increased with increasing water content, from $\Delta H = 25$ kJmol^{-1} in pure $(CD_3)_2CO$ to 39 kJmol^{-1} in 0.91:0.09 D_2O:$(CD_3)_2CO$, before dropping again to 20 kJmol^{-1} in pure D_2O. These data can be interpreted as a competition between the stabilization of the low-spin state by hydrogen bonding to D_2O; and, hydrolysis of the labile high-spin form which is more prevalent at higher D_2O concentrations (the hydrolysis is a pre-equilibrium to the spin-crossover event, which leads to an increased ΔH value for the combined process [51]). These results were confirmed by room temperature UV/vis spectra, which showed a perfect correlation between the low-spin MLCT ε_{max}, and the low-spin fraction of the sample at 298 K according to the susceptibility measurements [46].

These results explain the unusual stability of $[Fe(3-bpp)_2]^{2+}$ in aqueous solution, since hydrogen bonding between the complex and that solvent increases $T_{1/2}$ above room temperature. Thus *ca.* 65 % of the sample is in its low-spin state under ambient conditions, which is kinetically inert to hydrolysis. This stability only occurs in pure water, however; in acetone:water mixtures $T_{1/2}$ is lower and the majority of the sample adopts the high-spin state at room temperature, which is much more sensitive to ligand displacement and substitution. These observations have recently been confirmed by Harris *et al.*, who investigated [Fe(3-bpp)$_2$]$^{2+}$ as a temperature-dependent probe for MRI measurements [52].

3.3 Anion dependence

Following this study, we measured six different salts of $[Fe(3\text{-}bpp)_2]X_2$ ($X^- = BPh_4^-$, BF_4^-, $CF_3SO_3^-$, NCS^-, NO_3^- and Br^-) in a fixed 0.1:0.9 D_2O:$(CD_3)_2CO$ solvent composition, in which all of these salts were soluble to some degree [53]. While the thiocyanate salt showed clear evidence of ligand redistribution reactions in solution, the results with the other anions confirmed Goodwin's original data, with a perfect correlation between $T_{1/2}$ and Lungwitz and Spange's β^N parameter which is proportional to the hydrogen bond donor strength of the anion (Fig. 10) [54]. This was confirmed by titration of Br^- into $[Fe(3\text{-}bpp)_2][BPh_4]_2$, which afforded an approximately linear relationship between $T_{1/2}$ and the bromide concentration. The increase in $T_{1/2}$ caused by addition of 2 equivalents of Br^- is only 15 K. However, because $T_{1/2}$ is close to room temperature, this small change in $T_{1/2}$ leads to a 0.35 $cm^3mol^{-1}K$ reduction in $\chi_M T$ at 293 K in the presence of Br^-, which is comparable to the room temperature response to halide ions in Shores' systems [40]. In any case, the observation of any influence of different anions on $T_{1/2}$ in such a competitive aqueous solvent mixture implies that ion pairing and hydrogen bonding in $[Fe(3\text{-}bpp)_2]^{2+}$ salts is notably strong [55].

<Insert Figure 10 here>

3.4 Number of hydrogen bond donors

Susceptibility data for $[Fe(3\text{-}bpp)_2][BF_4]_2$ and $[Fe(1\text{-}bpp)_2][BF_4]_2$ in $(CD_3)_2CO$ are superimposable, implying that hydrogen bonding to this weakly interacting solvent has a negligible effect on the spin state of $[Fe(3\text{-}bpp)_2]^{2+}$. Interestingly, however, $[Fe(1,3\text{-}bpp)_2][BF_4]_2$ (Scheme 1) undergoes spin-crossover with a slightly higher midpoint temperature under the same conditions, showing $T_{1/2} = 254\pm1$ K in $(CD_3)_2CO$ (Fig. 11) [38].

The difference reflects a reduced ΔH and ΔS of spin-crossover for $[Fe(1,3\text{-bpp})_2]^{2+}$, which are both *ca.* 15 % lower than for the symmetric complexes according to van't Hoff plots (Table 1). We suggest this may be caused by a less ordered solvent sheath about the unsymmetric $[Fe(1,3\text{-bpp})_2]^{2+}$ cation, which would then undergo a smaller rearrangement during its spin-crossover equilibrium. The small stabilization of the low-spin state in $[Fe(1,3\text{-bpp})_2][BF_4]_2$ is consistent with its solid state properties, since the crystalline compound is low-spin at room temperature and below [38].

<Insert Figure 11 and Table 1 here>

As mentioned previously, salts of $[Fe(1\text{-bpp})_2]^{2+}$ decompose immediately in water, precipitating the colorless free ligand. In contrast, $[Fe(1,3\text{-bpp})_2][BF_4]_2$ retains its brown coloration when added to water, implying it is also water-stable. However, this could not be quantified by Evans method because of the poor solubility of $[Fe(1,3\text{-bpp})_2]^{2+}$ salts in aqueous solution.

3.5 Enhancing the Hydrogen Bonding Capabilities of $[Fe(3\text{-bpp})_2]^{2+}$

In the light of these encouraging results, we sought to modify $[Fe(3\text{-bpp})_2]^{2+}$ to improve its hydrogen bonding properties, and maximize the influence of host:guest interactions on its spin state. We pursued this by introducing additional hydrogen bond-donor groups adjacent to the pyrazolyl NH functions in 3-bpp (L^1 and L^2R; Scheme 4); by placing hydrophobic substituents in the same positions, to enhance N−H…X^- hydrogen bonding to X^- counterions (L^3R, L^4Me); and a combination of the two (L^4NH_2). We have had previous success using both those strategies to promote supramolecular assembly structures in other metal complexes of *N*H pyrazoles [56] and pyrazolyl chelate ligands [57]. The ligands L^4R are

noteworthy, as the first unsymmetrically substituted derivatives of the 3-bpp ligand type [1] (1-bpp derivatives with an unsymmetric distribution of pyrazole substituents are easier to obtain [58]).

<Insert Scheme 4 here>

The most interesting compounds we have studied thus far, from the point of view of spin-crossover, are the salts of the simplest ligand derivative $[Fe(L^3Me)_2]Y_2$ ($Y^- = BF_4^-$ and ClO_4^-). Both salts afford anhydrous crystals when freshly prepared, which rapidly convert to isostructural dihydrate phases on exposure to air. The dihydrate materials contain a mixture of high-spin and low-spin complex cations, which are hydrogen bonded to the Y^- anions and the lattice water respectively. That is consistent with the aforementioned stabilization of the low-spin state of $[Fe(3-bpp)_2]^{2+}$ salts by hydrogen bonding to water. Annealing both $[Fe(L^3Me)_2]Y_2 \cdot 2H_2O$ compounds *in vacuo* at 350 K affords new $[Fe(L^3Me)_2]Y_2$ anhydrous materials, that are again isostructural but are distinct from the original crystals. The annealed BF_4^- salt undergoes a sequence of three phase changes on cooling, culminating in an abrupt spin-transition around 205 K with a pronounced hysteresis loop ($\Delta T_{1/2}$ = 37-65 K depending on the history of the sample) [17]. In contrast the ClO_4^- salt only exhibits the first of the above crystallographic phase changes after annealing, and remains high-spin between 3-350 K; evidently the second phase change in the BF_4^- salt is required to activate it towards spin-crossover [59]. Since most of these transitions were monitored *in situ* by X-ray powder diffraction, the structural detail underlying this unprecedented phase behaviour is unclear at the time of writing. However, the structures of the precursor phases imply that disorder of the Y^- anions between hydrogen bonding sites on different cations may occur in the annealed materials, and could play an important role in their structural complexity [59].

Salts of $[Fe(L^1)_2]^{2+}$, $[Fe(L^2tBu)_2]^{2+}$, $[Fe(L^3tBu)_2]^{2+}$ and $[Fe(L^4Me)_2]^{2+}$ were all crystallographically characterized, and show extensive N−H…Y^- hydrogen bonding to the Y^- counterions and or solvent as expected (Fig. 12) [60]. Some of the compounds form unusual hydrogen bond network topologies, including $[Fe(L^1)_2][ClO_4]_2 \cdot 2(C_2H_5)_2O \cdot CH_3NO_2$ (an eight-connected fluorite {**flu**} topology) and $[Fe(L^3tBu)_2][BF_4]_2 \cdot xCF_3CH_2OH \cdot y(C_3H_7)_2O$ (a helical self-penetrating network derived from the (10,3)-a {**srs**} net) [63]. However in the solid state they are all either high-spin, or show very poorly defined spin-crossover on cooling [60]. Solutions of $[Fe(L^1)_2]^{2+}$, $[Fe(L^2tBu)_2]^{2+}$, $[Fe(L^3tBu)_2]^{2+}$, $[Fe(L^4Me)_2]^{2+}$ and $[Fe(L^4NH_2)_2]^{2+}$ are high-spin in $(CD_3)_2CO$ at room temperature, but all of them except $[Fe(L^2tBu)_2]^{2+}$ exhibit the onset of spin-crossover on cooling (Fig. 13). The $T_{1/2}$ values for $[Fe(L^1)_2]^{2+}$ (*ca.* 190 K) and $[Fe(L^4Me)_2]^{2+}$ (218 K) are within the liquid range of the solvent, but for the other complexes it is significantly lower. Stabilization of the high-spin state in $[Fe(3\text{-}bpp)_2]^{2+}$ derivatives by electron-donating amino and alkyl substituents is unexpected at first glance, and is the opposite trend to analogous complexes from the $[Fe(1\text{-}bpp)_2]^{2+}$ series, substituted at the pyrazolyl $C4$ sites [64]. A theoretical study to address this anomaly is in progress at the time of writing.

<Insert Figures 12 and 13 here>

Since $[Fe(L^1)_2][ClO_4]_2$ hydrolyzes in aqueous solution, any stabilization of its low-spin state by hydrogen bonding in water is insufficient to raise $T_{1/2}$ above room temperature (which would require an increase in $T_{1/2}$ almost twice as large as observed in $[Fe(3\text{-}bpp)_2]^{2+}$). It is also unique among the compounds in this article in being sensitive to aerobic oxidation [60]. That can be attributed to reduction of the Fe(II/III) potential by the donating amino substituents, combined with the acidity of the L^1 N−H functions (which may be deprotonated following oxidation of the iron center [65]).

4. Conclusion

This report has described two different studies, which each advance our understanding of the spin-states of $[Fe(1-bpp)_2]^{2+}$, $[Fe(3-bpp)_2]^{2+}$ and their derivatives. First, is a new survey of the crystal structures of $[Fe(1-bpp)_2]^{2+}$ complexes, published during the last twelve years (and including some unpublished examples from the Halcrow group [38]). The analysis has rationalized the unusual coordination geometries exhibited by many of these compounds (Figs. 1 and 2), which arise from a tension between two factors: the typical Bailar twist (octahedron→trigonal prism) distortion that is often found in six-coordinate complexes; and, the narrow clamp angle of the 1-bpp ligand (Scheme 3), which causes the geometries to deviate from the ideal Bailar twist pathway. The most distorted coordination geometries correlate strongly with the presence of additional intermolecular contacts from anions or neighboring ligand substituents to the iron center. Therefore, while the electronic origin of the high-spin distortion is the Jahn-Teller effect, the wide variety of distorted structures that have been observed in this series of compounds is controlled by crystal packing effects. This conclusion will be of great value for interpreting the stereochemistries of $[Fe(1-bpp)_2]^{2+}$ and $[Fe(3-bpp)_2]^{2+}$ compounds [2, 3], as well as other complexes showing this type of Jahn-Teller distortion [21]. The degree of distortion in a high-spin $[Fe(1-bpp)_2]^{2+}$ complex salt correlates with the cooperativity of its spin-transition, as well as determining whether it undergoes spin-crossover in the first place [2]. Hence, this new understanding of the distortion also has wider implications for the crystal engineering of new spin-transition materials [7].

Second, we have described recent work that addresses how hydrogen bonding to the NH groups in $[Fe(3-bpp)_2]^{2+}$ controls its spin-crossover properties. The temperature of the spin-

crossover equilibrium for $[Fe(3\text{-bpp})_2]^{2+}$ in solution increases measurably in more donating organic solvents, and is especially sensitive to the presence of water [46]. Spin-crossover measurements of $[Fe(3\text{-bpp})_2]^{2+}$ can also detect the presence of different counter-anions, even in a relatively polar water:acetone solvent mixture [53]. The only comparable literature study is on $[Fe(tacn)_2]^{2+}$, which is less sensitive to its local environment than $[Fe(3\text{-bpp})_2]^{2+}$ despite having more NH groups per molecule [50]. We explain this from the increased acidity of the pyrazolyl NH groups in $[Fe(3\text{-bpp})_2]^{2+}$, compared to the secondary amino NH groups in $[Fe(tacn)_2]^{2+}$ (the acidic pK_a values for uncoordinated $1H$-pyrazole and secondary amine NH groups are *ca.* 14 [66] and 35 [67], respectively). For this reason, the NH groups in $[Fe(3\text{-bpp})_2]^{2+}$ are more polarizable than in $[Fe(tacn)_2]^{2+}$, and its hydrogen bonds will be stronger. The importance of the second coordination sphere in these measurements was illustrated by the unsymmetric analogue $[Fe(1,3\text{-bpp})_2]^{2+}$, which undergoes spin-crossover at a higher temperature than the symmetric complexes $[Fe(1\text{-bpp})_2]^{2+}$ and $[Fe(3\text{-bpp})_2]^{2+}$ in $(CD_3)_2CO$ solution (Table 1).

Attempts to augment the supramolecular response of spin-crossover in $[Fe(3\text{-bpp})_2]^{2+}$ by modification of the 3-bpp ligand have led to some interesting solid state structures [60] and crystallographic phase behavior [17, 59], but have not yet led to supramolecular spin-state switching in solution. Our current challenge is to design new modifications to the $[Fe(3\text{-bpp})_2]^{2+}$ framework that enhance its hydrogen bonding capabilities, while keeping its spin-state equilibrium close to room temperature.

Supplementary data

Synthetic procedures, analytical characterization and crystallographic data for $[Fe(1,3-bpp)_2][BF_4]_2$, and for unpublished $[Fe(1-bpp)_2]^{2+}$ derivatives that were included in the shape measures analysis. The crystallographic data are available on request from the Cambridge Crystallographic Data Centre, 12 Union Road, Cambridge CB2 1EZ, UK (http://www.ccdc.cam.ac.uk/). The CCDC deposition numbers are 1004453-1004457 and 1004459-1004460.

References

[1]   a) M. A. Halcrow, Coord. Chem. Rev. 249 (2005) 2880;

b) J. Olguín, S. Brooker, Coord. Chem. Rev. 255 (2011) 203;

c) M. A. Halcrow, New J. Chem. 38 (2014) 1868.

[2]   M. A. Halcrow, Coord. Chem. Rev. 253 (2009) 2493.

[3]   G. A. Craig, O. Roubeau, G. Aromí, Coord. Chem. Rev. 269 (2014) 13.

[4]   a) P. Gütlich, H. A. Goodwin (Eds.), Spin Crossover in Transition Metal Compounds I-III − Top. Curr. Chem. vols. 233-235, Springer Verlag, Berlin, Germany, 2004.

b) M. A. Halcrow (Ed.), Spin-crossover materials – properties and applications, John Wiley & Sons, Chichester, UK, 2013.

[5]   Recent reviews of the applications and nanoscience of spin-crossover materials:

a) A. Bousseksou, G. Molnár, L. Salmon, W. Nicolazzi, Chem. Soc. Rev. 40 (2011) 3313;

b) M. Cavallini, Phys. Chem. Chem. Phys. 14 (2012) 11867;

c) H. J. Shepherd, G. Molnár, W. Nicolazzi, L. Salmon, A. Bousseksou, Eur. J. Inorg. Chem. (2013) 653;

d) G. Molnár, L. Salmon, W. Nicolazzi, F. Terki, A. Bousseksou, J. Mater. Chem. C 2 (2014) 1360.

[6]   Recent reviews of other aspects of spin-crossover compounds:

a) M. C. Muñoz, J. A. Real, Coord. Chem. Rev. 255 (2011) 2068;

b) J. Tao, R.-J. Wei, R.-B. Huang, L.-S. Zheng, Chem. Soc. Rev. 41 (2012) 703;

c) P. Gütlich, Eur. J. Inorg. Chem. (2013) 581;

d) S. Hayami, M. R. Karim,Y. H. Lee, Eur. J. Inorg. Chem. (2013) 683;

e) P. Gütlich, A. B. Gaspar, Y. Garcia, Beilstein J. Org. Chem. 9 (2013) 342;

f) M. Sorai, Y. Nakazawa, M. Nakano, Y. Miyazaki, Chem. Rev. 113 (2013) PR41;

g) P. Guionneau, Dalton Trans. 43 (2014) 382;

h) A. B. Gaspar, M. Seredyuk, Coord. Chem. Rev. 268 (2014) 41.

[7] M. A. Halcrow, Chem. Soc. Rev. 40 (2011) 4119.

[8] J. M. Holland, S. A. Barrett, C. A. Kilner, M. A. Halcrow, Inorg. Chem. Commun. 5 (2002) 328.

[9] a) C. Rajadurai, O. Fuhr, R. Kruk, M. Ghafari, H. Hahn, M. Ruben, Chem. Commun. (2007) 2636;

b) J. Elhaïk, C. M. Pask, C. A. Kilner, M. A. Halcrow, Tetrahedron 63 (2007) 291;

c) C. A. Tovee, C. A. Kilner, S. A. Barrett, J. A. Thomas, M. A. Halcrow, Eur. J. Inorg. Chem. (2010) 1007.

[10] M. Nihei, N. Takahashi, H. Nishikawa and H. Oshio, Dalton Trans. 40 (2011) 2154.

[11] R. González-Prieto, B. Fleury, F. Schramm, G. Zoppellaro, R. Chandrasekar, O. Fuhr, S. Lebedkin, M. Kappes, M. Ruben, Dalton Trans. 40 (2011) 7564.

[12] Y. Hasegawa, K. Takahashi, S. Kume, H. Nishihara, Chem. Commun. 47 (2011) 6846;

b) K. Takahashi, Y. Hasegawa, R. Sakamoto, M. Nishikawa, S. Kume, E. Nishibori, H. Nishihara, Inorg. Chem. 51 (2012) 5188.

[13] M. Nihei, T. Maeshima, Y. Kose, H. Oshio, Polyhedron 26 (2007) 1993.

[14] a) M. Nihei, L. Han, H. Oshio, J. Am. Chem. Soc. 129 (2007) 5312;

b) M. Nihei, L. Han, H. Tahira, H. Oshio, Inorg. Chim. Acta 361 (2008) 3926.

[15] a) M. S. Alam, M. Stocker, K. Gieb, P. Müller, M. Haryono, K. Student, A. Grohmann, Angew. Chem. Int. Ed. 49 (2010) 1159;

b) D. Secker, S. Wagner, S. Ballmann, R. Härtle, M. Thoss, H. B. Weber, Phys. Rev. Lett. 106 (2011) 136807/1;

c) V. Meded, A. Bagrets, K. Fink, R. Chandrasekar, M. Ruben, F. Evers, A. Bernand-Mantel, J. S. Seldenthuis, A. Beukman, H. S. J. van der Zant, Phys. Rev. B 83 (2011) 245415/1.

[16] a) T. D. Roberts, M. A. Little, L. J. Kershaw Cook, S. A. Barrett, F. Tuna, M. A. Halcrow, Polyhedron 64 (2013) 4;

b) T. D. Roberts, M. A. Little, L.J. Kershaw Cook, M. A. Halcrow, Dalton Trans. 43 (2014) 7577.

[17] T. D. Roberts, F. Tuna, T. L. Malkin, C. A. Kilner, M. A. Halcrow, Chem. Sci. 3 (2012) 349.

[18] a) G. A. Craig, J. S. Costa, O. Roubeau, S. J. Teat, G. Aromí, Chem. Eur. J. 17 (2011) 3120;

b) G. A. Craig, J. S. Costa, S. J. Teat, O. Roubeau, D. S. Yufit, J. A. K. Howard, G. Aromí, Inorg. Chem. 52 (2013) 7203;

c) Gavin A. Craig, J. S. Costa, O. Roubeau, S. J. Teat, H. J. Shepherd, M. Lopes, G. Molnár, A. Bousseksou, G. Aromí, Dalton Trans. 43 (2014) 729;

[19] J. S. Costa, S. Rodríguez-Jiménez, G. A. Craig, B. Barth, C. M. Beavers, S. J. Teat, G. Aromí, J. Am. Chem. Soc. 136 (2014) 3869.

[20] a) T. Buchen, P. Gütlich, H. A. Goodwin, Inorg. Chem. 33 (1994) 4573;

b) T. Buchen, P. Gütlich, K. H. Sugiyarto, H. A. Goodwin, Chem. Eur. J. 2 (1996) 113;

c) A. Bhattacharjee, V. Ksenofontov, K. H. Sugiyarto, H. A. Goodwin, P. Gütlich, Adv. Funct. Mater. 13 (2003) 877;

d) K. H. Sugiyarto, W.-A. McHale, D. C. Craig, A. D. Rae, M. L. Scudder, H. A. Goodwin, DaltonTrans. (2003) 2443;

d) C. M. Grunert, H. A. Goodwin, C. Carbonera, J.-F. Létard, J. Kusz, P. Gütlich, J. Phys. Chem. B 111 (2007) 6738.

[21] See *e.g.*

a) E. C. Constable, G. Baum, E. Bill, R. Dyson, R. van Eldik, D. Fenske, S. Kaderli, D. Morris, A. Neubrand, M. Neuburger, D. R. Smith, K. Wieghardt, M. Zehnder and A. D. Zuberbühler, Chem. Eur. J. 5 (1999) 498;

b) C. W. Glynn, M. M. Turnbull, Transition Met. Chem. 27 (2002) 822;

c) F. Pelascini, M. Wesolek, F. Peruch, A. De Cian, N. Kyritsakas, P. J. Lutz, J. Kress, Polyhedron 23 (2004) 3193;

d) G. Stupka, L. Gremaud, G. Bernardinelli, A. F. Williams, Dalton Trans. (2004) 407;

e) B. S. Hammes, B. J. Damiano, P. H. Tobash, M. J. Hidalgo, G. P. A. Yap, Inorg. Chem. Commun. 8 (2005) 513;

f) S. Y. Brauchli, E. C. Constable, K. Harris, D. Häussinger, C. E. Housecroft, P. J. Rösel, J. A. Zampese, Dalton Trans. 39 (2010) 10739.

[22] J. M. Holland, J. A. McAllister, C. A. Kilner, M. Thornton-Pett, A. J. Bridgeman, M. A. Halcrow, J. Chem. Soc. Dalton Trans. (2002) 548.

[23] J. Elhaïk, D. J. Evans, C. A. Kilner, M. A. Halcrow, Dalton Trans. (2005) 1693.

[24] J. Elhaïk, C. A. Kilner, M. A. Halcrow, Dalton Trans. (2006) 823.

[25] a) J. Elhaïk, C. A. Kilner, M. A. Halcrow, CrystEngComm 7 (2005) 151;
b) C. A. Kilner, M. A. Halcrow, Polyhedron 25 (2006) 235;
c) M. Haryono, F. W. Heinemann, K. Petukhov, K. Gieb, P. Müller, A. Grohmann, Eur. J. Inorg. Chem. (2009) 2136.

[26] a) Y. Hasegawa, R. Sakamoto, K. Takahashi, H. Nishihara, Inorg. Chem. 52 (2013) 1658;
b) L. J. Kershaw Cook, F. Thorp-Greenwood, H. J. Shepherd, O. Cespedes, T. P. Comyn, M. A. Halcrow, in preparation;
c) L. J. Kershaw Cook, H. J. Shepherd, O. Cespedes, T. P. Comyn, G. Chastanet, J.-F. Létard, M. A. Halcrow, in preparation.

[27] a) M. Clemente-León, E. Coronado, M. C. Giménez-López, F. M. Romero, Inorg. Chem. 46 (2007) 11266;

b) G. A. Craig, J. S. Costa, O. Roubeau, S. J. Teat, G. Aromí, Chem. Eur. J. 18 (2012) 11703.

[28] M. Pinsky, D. Avnir, Inorg. Chem. 37 (1998) 5575.

[29] S. Alvarez, P. Alemany, D. Casanova, J. Cirera, M. Llunell, D. Avnir, Coord. Chem. Rev. 249 (2005) 1693.

[30] S. Alvarez, E. Ruiz, in: J. W. Steed, P. A. Gale (Eds.), Supramolecular Chemistry, From Molecules to Nanomaterials, John Wiley & Sons, Chichester, UK, 2012, vol. 5, pp. 1993−2044.

[31] M. Llunell, D. Casanova, J. Cirera, P. Alemany, S. Alvarez, SHAPE v. 2.1, University of Barcelona (2013).

[32] S. Alvarez, J. Am. Chem. Soc. 125 (2003) 6795.

[33] D. Casanova, J. Cirera, M. Llunell, P. Alemany, D. Avnir, S. Alvarez. J. Am. Chem. Soc. 126 (2004) 1755.

[34] S. Alvarez, D. Avnir, M. Llunell, M. Pinsky, New J. Chem. 26 (2002) 996.

[35] J. C. Bailar jr., J. Inorg. Nucl. Chem. 8 (1958) 165.

[36] J. Cirera, E. Ruiz, S. Alvarez, Chem. Eur. J. 12 (2006) 3162.

[37] J.-F. Létard, J. Mater. Chem. 16 (2006) 2550.

[38] Some previously unpublished structures of $[Fe(1\text{-}bpp)_2]^{2+}$ derivatives, and of $[Fe(1,3\text{-}bpp)_2]^{2+}$, were included in this analysis. Synthetic procedures and analytical and crystallographic data for those compounds are given in the Supporting Information.

[39] A. Ruiz-Martínez, D. Casanova, S. Alvarez, Chem. Eur. J. 16 (2010) 6567.

[40] a) Z. Ni, M. P. Shores, J. Am. Chem. Soc. 131 (2009) 32;
      b) Z. Ni, M. P. Shores, Inorg. Chem. 49 (2010) 10727;
      c) Z. Ni, A. M. McDaniel, M. P. Shores, Chem. Sci. 1 (2010) 615;
      d) Z. Ni, S. R. Fiedler, M. P. Shores, Dalton Trans. 40 (2011) 944.

[41] a) M. C. Young, E. Liew, J. Ashby, K. E. McCoy, R. J. Hooley, Chem. Commun. 49 (2013) 6331;
      b) M. C. Young, E. Liew, R. J. Hooley, Chem. Commun. 50 (2014) 5043.

[42] a) K. H. Sugiyarto, H. A. Goodwin, Aust. J. Chem. 41 (1988) 1645;
      b) K. H. Sugiyarto, M. L. Scudder, D. C. Craig, H. A. Goodwin, Aust. J. Chem. 53 (2000) 755.

[43] K. H. Sugiyarto, D. C. Craig, A. D. Rae, H. A. Goodwin, Aust. J. Chem. 47 (1994) 869.

[44] a) T. Buchen, P. Gütlich and H. A. Goodwin, Inorg. Chem. 33 (1994) 4573;

b) T. Buchen, P. Gütlich, K. H. Sugiyarto, H. A. Goodwin, Chem. Eur. J. 2 (1996) 1134;

c) K. H. Sugiyarto, W.-A. McHale, D. C. Craig, A. D. Rae, M. L. Scudder, H. A. Goodwin, Dalton Trans. (2003) 2443.

[45] a) M. L. Scudder, D. C. Craig, H. A. Goodwin, CrystEngComm 7 (2005) 642;

b) E. Coronado, M. C. Giménez-López, C. Giménez-Saiz, F. M. Romero, CrystEngComm 11 (2009) 2198;

c) M. Clemente-León, E. Coronado, M. C. Giménez-López, F. M. Romero, S. Asthana, C. Desplanches, J.-F. Létard, Dalton Trans. (2009) 8087.

[46] S.A. Barrett, C. A. Kilner, M. A. Halcrow, Dalton Trans. 40 (2011) 12021.

[47] a) V. Gutmann, D. Wychera, Inorg. Nucl. Chem. Lett 2 (1966) 257;

b) Y. Marcus, Chem. Soc. Rev. 22 (1993) 409.

[48] M. J. Kamlet, J.-L. M. Abboud, M. H. Abraham, R. W. Taft, J. Org. Chem. 48 (1983) 2877.

[49] a) M. A. Hoselton, L. J. Wilson, R. S. Drago, J. Am. Chem. Soc. 97 (1975) 1722;

b) M. F. Tweedle, L. J. Wilson, J. Am. Chem. Soc. 98 (1976) 4824;

c) M. G. Simmons, L. J. Wilson, Inorg. Chem. 16 (1977) 126;

d) B. Strauβ, V. Gutmann, W. Linert, Monatsh. Chem. 124 (1993) 515;

e) W. Linert, M. Enamullah, V. Gutmann, R. F. Jameson, Monatsh. Chem. 125 (1994) 661;

f) L. L. Martin, R. L. Martin, A. M. Sargeson, Polyhedron 13 (1994) 1969.

[50]   J. W. Turner, F. A. Schultz, Inorg. Chem. 40 (2001) 5296.

[51]   a) M. Enamullah, W. Linert, Thermochim. Acta 388 (2002) 401;

b) K. P. Bryliakov, E. A. Duban, E. P. Talsi, Eur. J. Inorg. Chem. (2005) 72.

[52]   I.-R. Jeon, J. G. Park, C. R. Haney, T. D. Harris, Chem. Sci. 5 (2014) 2461.

[53]   S. A. Barrett, M. A. Halcrow, RSC Adv. 4 (2014) 11240.

[54]   R. Lungwitz, S. Spange, New J. Chem. 32 (2008) 392.

[55]   S. Kubik, Chem. Soc. Rev. 39 (2010) 3648.

[56]   a) X. Liu, A. C. McLaughlin, M. P. de Miranda, E. J. L. McInnes, C. A. Kilner, M. A. Halcrow, Chem. Commun. (2002) 2978;

b) X. Liu, J. A. McAllister, M. P. de Miranda, E. J. L. McInnes, C. A. Kilner, M. A. Halcrow, Chem. Eur. J. 10 (2004) 1827;

c) S. L. Renard, I. Sylvestre, S. A. Barrett, C. A. Kilner, M. A. Halcrow, Inorg. Chem. 45 (2006) 8711.

[57]   a) C. M. Pask, K. D. Camm, N. J. Bullen, M. J. Carr, W. Clegg, C. A. Kilner, M. A.

Halcrow, Dalton Trans. (2006) 662;

b) L. F. Jones, K. D. Camm, C. A. Kilner, M. A. Halcrow, CrystEngComm 8 (2006)

719;

c) L. F. Jones, S. A. Barrett, C. A. Kilner, M. A. Halcrow, Chem. Eur. J. 14 (2008)

223;

d) L. F. Jones, C. A. Kilner, M. A. Halcrow, Chem. Eur. J. 15 (2009) 4667;

e) J. J. Henkelis, L. F. Jones, C. A. Kilner, M. A. Halcrow, Inorg. Chem. 49 (2010)

11127;

f) J. J. Henkelis, C. A. Kilner, M. A. Halcrow, Chem. Commun. 47 (2011) 5187.

[58]   D. L. Jameson, K. A. Goldsby, J. Org. Chem. 55 (1990) 4992.

[59]   T. D. Roberts, M. A. Little, F. Tuna, C. A. Kilner, M. A. Halcrow, Chem. Commun.

49 (2013) 6280.

[60]   T. D. Roberts, M. A. Little, L. J. Kershaw Cook, M. A. Halcrow, Dalton Trans. 43

(2014) 7577.

[61]   K. A. Ali, ARKIVOC (2010) (xi) 55.

[62]   a) Y. Zhou, W. Chen, D. Wang, Dalton Trans. (2008) 1444;

b) A. Yoshinari, A. Tazawa, S. Kuwata, T. Ikariya, Chem. Asian J. 7 (2012) 1417.

33

[63]   L. Öhrströhm, K. Larsson, Molecule-Based Materials – the Structural Network Approach, Elsevier, Amsterdam, p. 314 (2005).

[64]   R. Pritchard, C. A. Kilner, S. A. Barrett, M. A. Halcrow, Inorg. Chim. Acta 362 (2009) 4365.

[65]   a) C. T. Brewer, G. Brewer, R. J. Butcher, E. E. Carpenter, A. M. Schmiedekamp, C. Viragh, Dalton Trans. (2007) 295;
b) D. Plaul, E. T. Spielberg, W. Plass, Z. Anorg. Allg. Chem. 636 (2010) 1268.

[66]   J. Catalan, M. Menendez, J. Elguero, Bull. Soc. Chim. France (1985) I-30.

[67]   R. R. Fraser, T. S. Mansour, J. Org. Chem. 49 (1984) 3442.

[68]   L. J. Barbour, J. Supramol. Chem. 1 (2003) 189.

[69]   POVRAY v. 3.5, Persistence of Vision Raytracer Pty. Ltd., Williamstown, Victoria, Australia (2002). http://www.povray.org.

[70]   SIGMAPLOT, v. 8.02, SPSS Scientific Inc., Chicago, IL, USA (2002).

[71]   C. R. Groom, F. H. Allen, Angew. Chem. Int. Ed. 53 (2014) 662.

Table 1. Spin-crossover parameters for the isomeric complexes [Fe(1-bpp)$_2$][BF$_4$]$_2$, [Fe(3-bpp)$_2$][BF$_4$]$_2$ and [Fe(1,3-bpp)$_2$][BF$_4$]$_2$ in (CD$_3$)$_2$CO solution.

	$T_{1/2}$, K	ΔH, kJmol^{-1}	ΔS, Jmol^{-1}K^{-1}	Ref
[Fe(1-bpp)$_2$][BF$_4$]$_2$	248(1)	24.1(2)	101(1)	[22]
[Fe(3-bpp)$_2$][BF$_4$]$_2$	247(1)	24.8(2)	100(1)	[46]
[Fe(1,3-bpp)$_2$][BF$_4$]$_2$	254(1)	22.0(2)	86(1)	This work
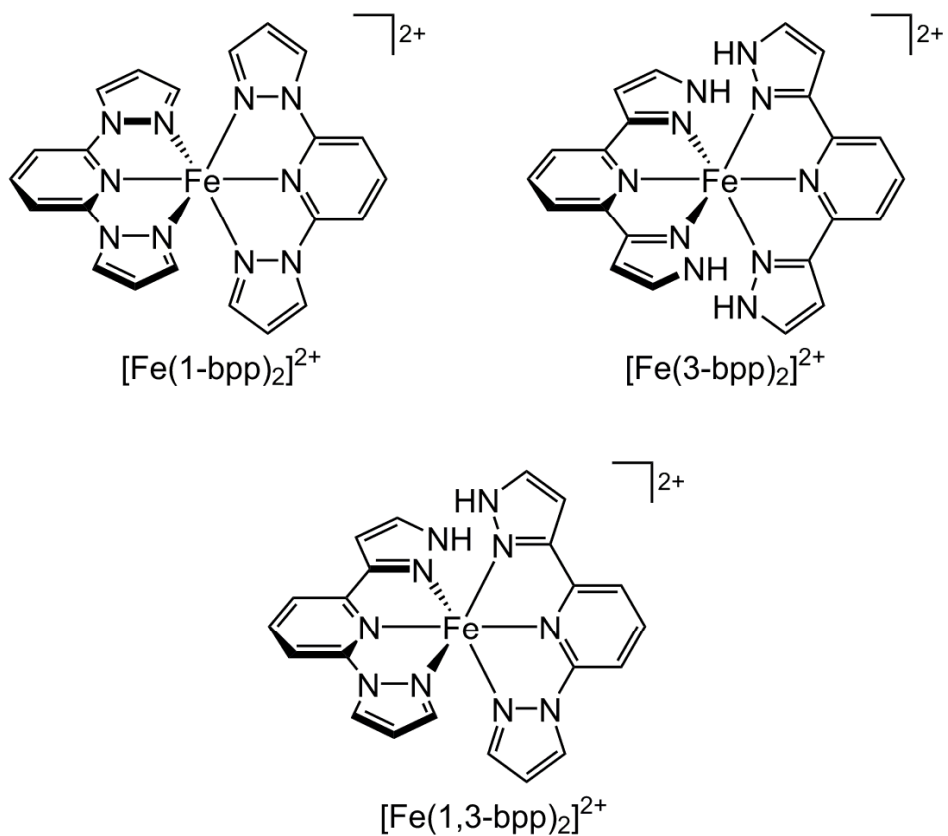
Scheme 1. The prototypical examples of the classes of complex referred to in this work.
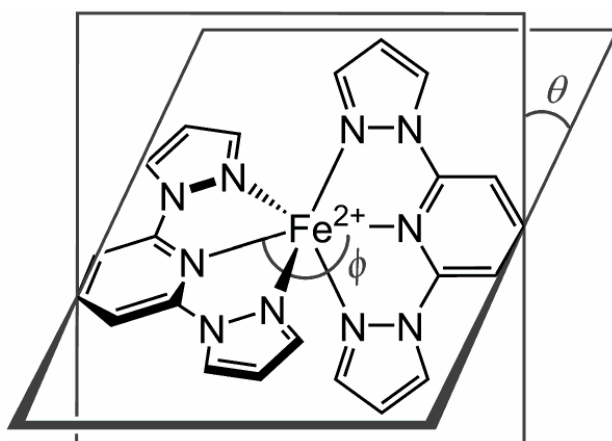
Scheme 2. The angular Jahn-Teller distortion exhibited by some high-spin $[Fe(1\text{-}bpp)_2]^{2+}$ and

$[Fe(3\text{-}bpp)_2]^{2+}$ derivatives ($\phi \leq 180°$, $\theta \leq 90°$).

36
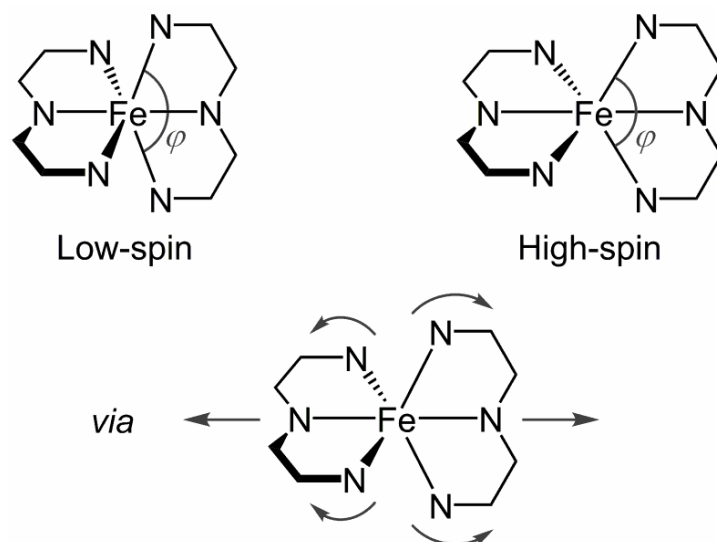
Scheme 3. The effect of a change in spin state on the internal clamp angle (φ) of a coordinated bpp-type ligand.
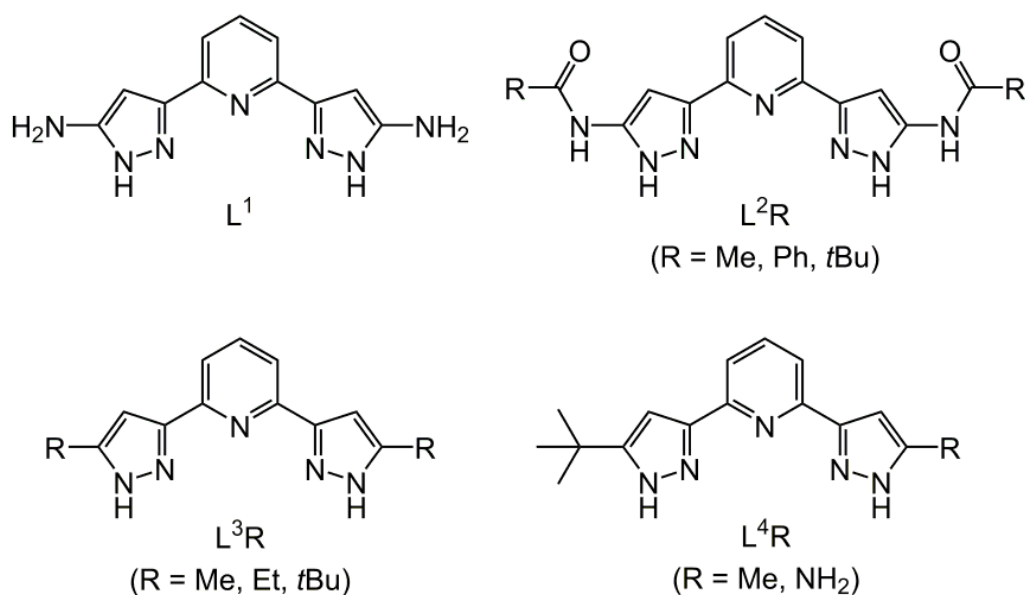
Scheme 4. Substituted 3-bpp derivatives we have investigated for spin-crossover chemistry [17, 59, 60]. Synthetic procedures for L^1 [61] and some L^3R derivatives [62] have been previously reported.
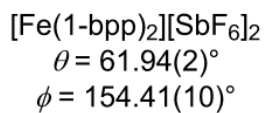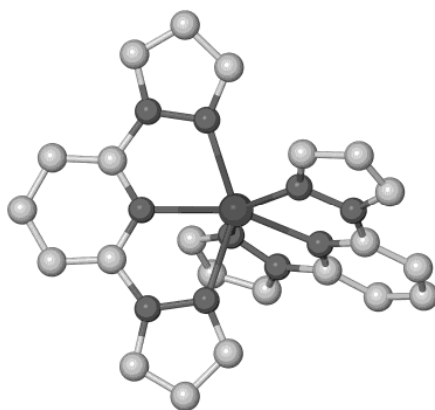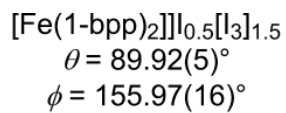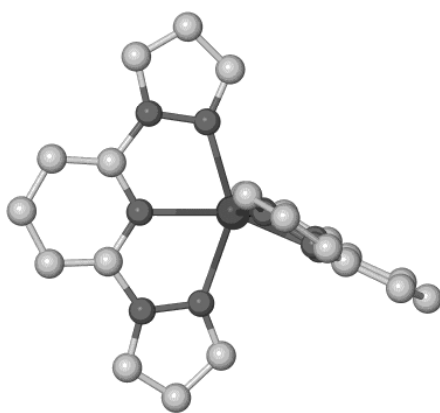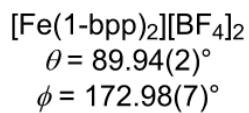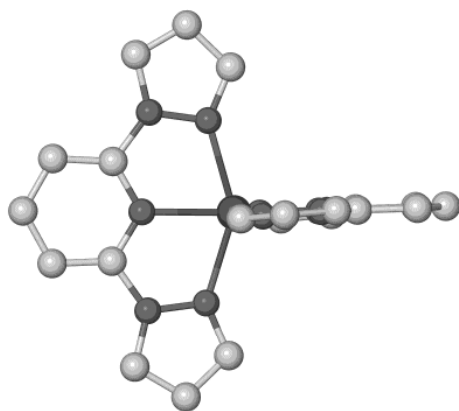
Fig. 1. High-spin crystal structures of three salts of $[Fe(1\text{-}bpp)_2]^{2+}$, illustrating the Jahn-Teller distortion [22-24]. Only the BF_4^- salt is spin-crossover active.
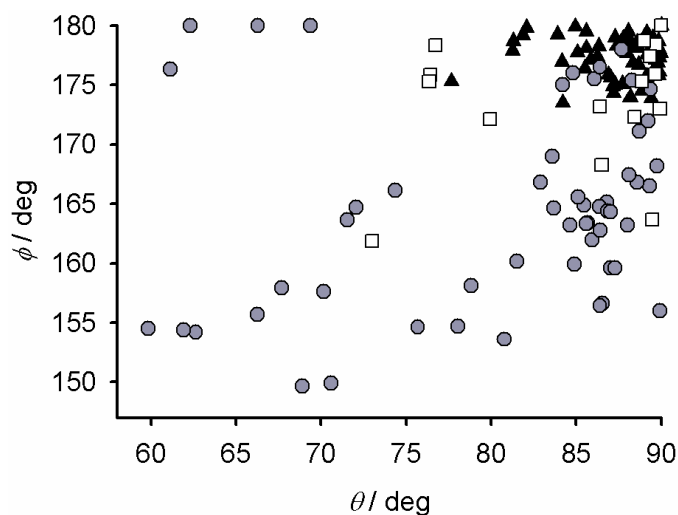
Fig. 2. The Jahn-Teller distortion parameters (Scheme 2) from crystal structures of [Fe(1-bpp)$_2$]$^{2+}$ complexes that are: low-spin (▲); high-spin and spin-crossover active (□); high-spin and spin-crossover inactive (●). This is an updated version of the equivalent figure in ref. [2].
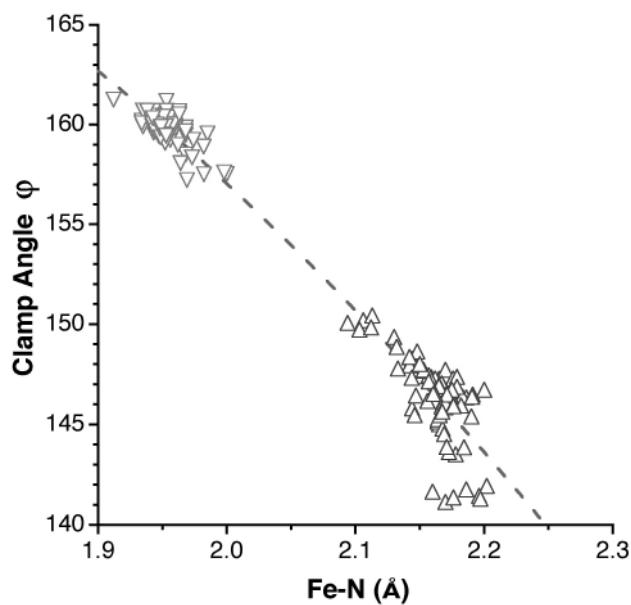
Fig. 3. Effect of the average Fe−N bond distance in [Fe(1-bpp)$_2$]$^{2+}$ complexes on the clamp angle φ (Scheme 3). High-spin molecules are plotted as upward triangles and low spin molecules as downward triangles.
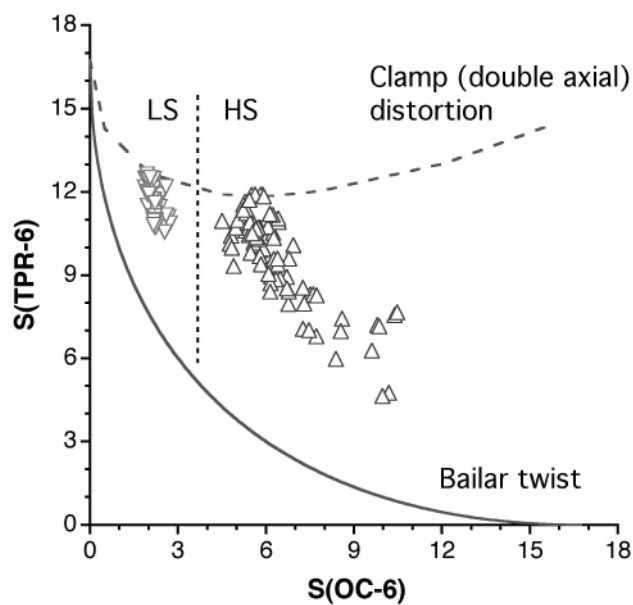
Fig. 4. Shape map of $[Fe(1\text{-}bpp)_2]^{2+}$ complexes relative to the octahedron (OC-6) and the trigonal prism (TPR-6). The Bailar twist and double axial distortion pathways (Scheme 3) of the octahedron are represented by a continuous and a dashed line, respectively. High-spin (HS) molecules are plotted as upward triangles and low spin (LS) molecules as downward triangles.
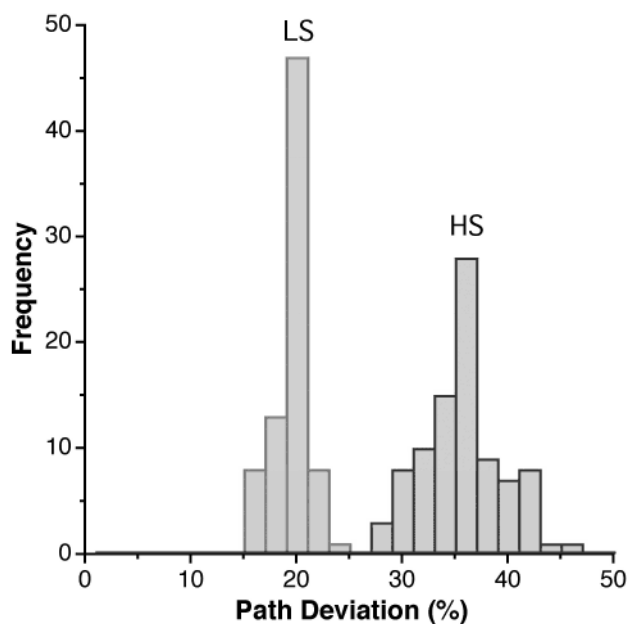
Fig. 5 Distribution of the deviations from the Bailar twist pathway for low-spin (LS) and high-spin (HS) $[Fe(1\text{-}bpp)_2]^{2+}$ complexes.
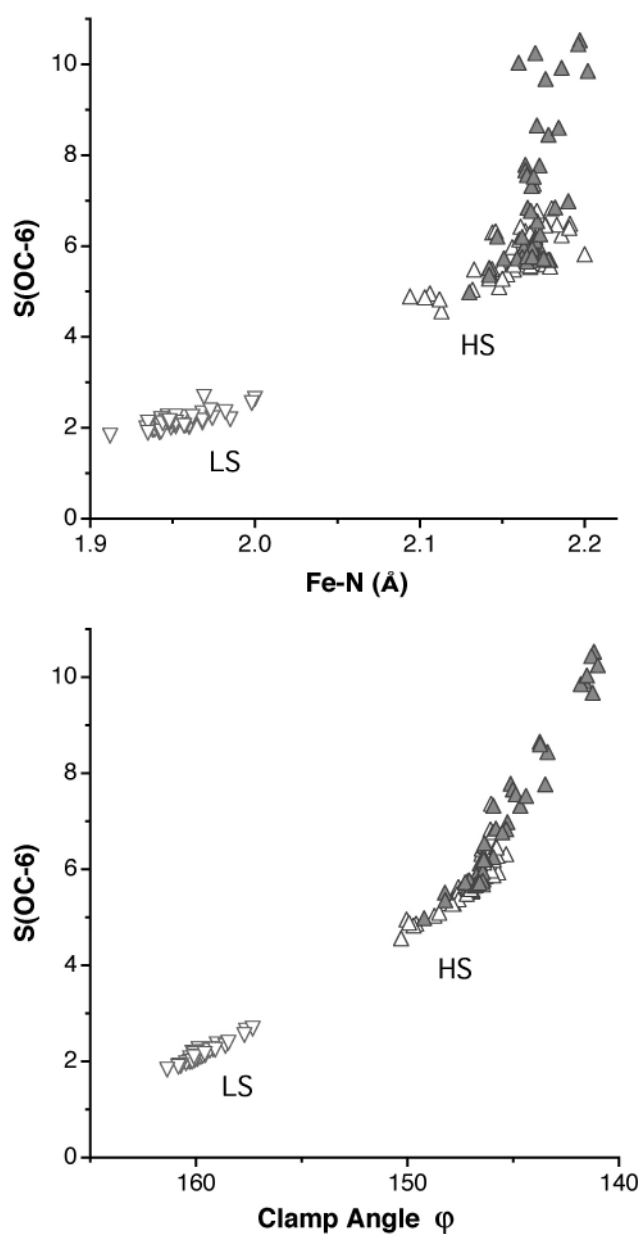
Fig. 6. Octahedral shape measures of the Fe atoms in $[Fe(1\text{-bpp})_2]^{2+}$ complexes, plotted as a function of their average Fe−N length (top), and their average clamp angle φ (bottom). Data corresponding to high-spin molecules are represented by upward triangles and low spin molecules by downward triangles. High-spin complexes with additional short intermolecular contacts to the iron center are shaded.
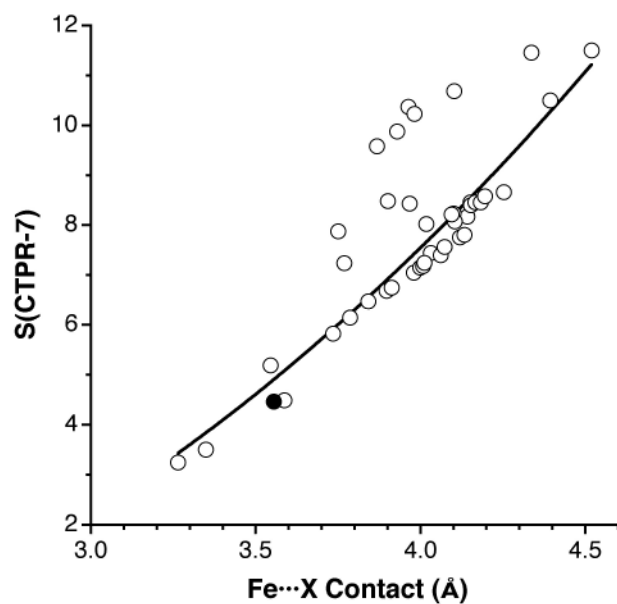
Fig. 7. Relationship between the capped trigonal prismatic shape measure of the FeN$_6$X core and the Fe…X distance for high spin [Fe(1-bpp)$_2$]$^{2+}$ molecules with short intermolecular contacts. The filled circle corresponds to the compound shown in Fig. 8.
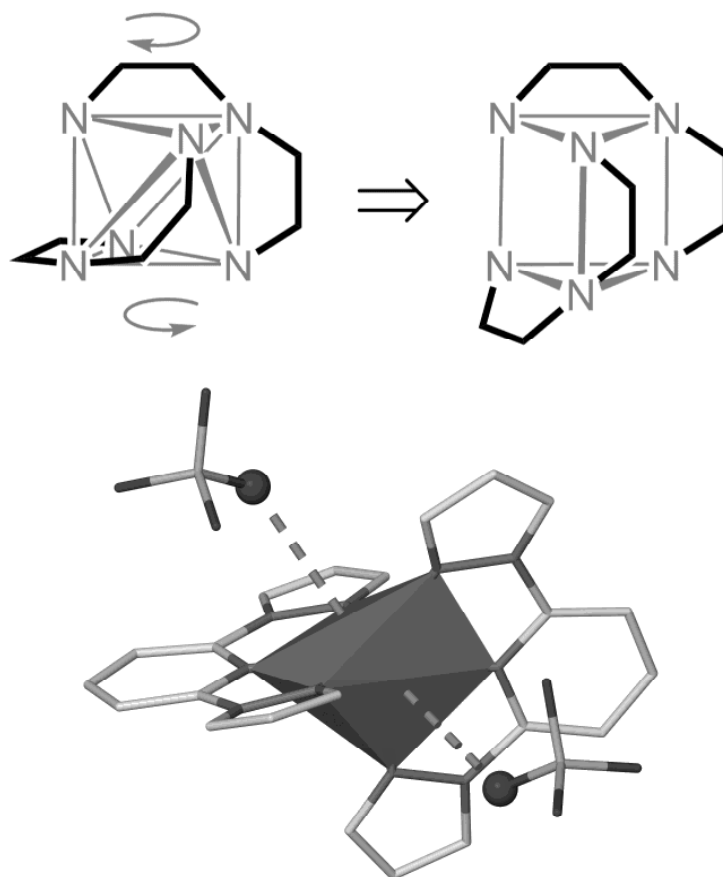
Fig. 8. Topology of the tridentate bpp ligands in the idealized trigonal prism coordination sphere that results from a Bailar twist (top), and the molecular structure of [Fe(1-bpp)$_2$][BF$_4$]$_2$ showing the distorted trigonal prismatic coordination sphere of the Fe atom and the oxygen atoms from two perchlorate anions that cap two rectangular faces (bottom).
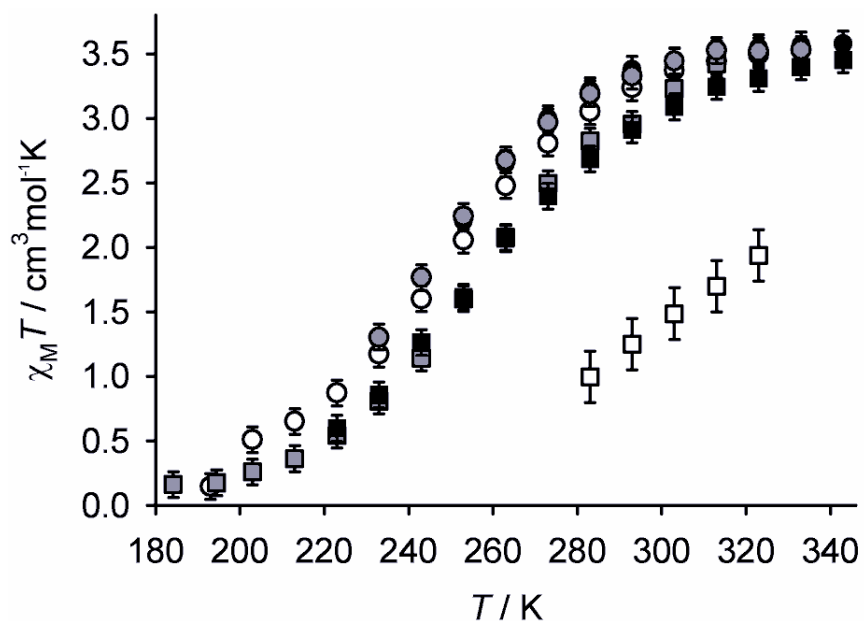
Fig. 9. Variable temperature magnetic susceptibility data for [Fe(3-bpp)$_2$][BF$_4$]$_2$ in CD$_3$NO$_2$ (●), CD$_3$CN (◕),{CD$_3$}$_2$CO (○), (CD$_3$)$_2$NCDO (■), CD$_3$OD (▣) and D$_2$O (□) [46].
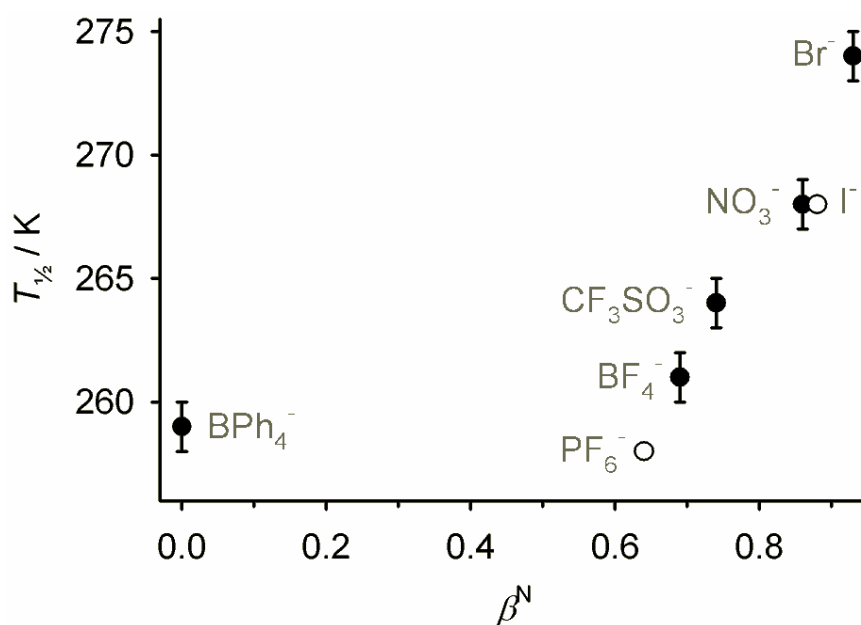
Fig. 10. Dependence of $T_{1/2}$ for [Fe(3-bpp)$_2$]X$_2$ on the hydrogen bonding power of different X$^-$ anions (β^N [54]), in a 0.1:0.9 D$_2$O:(CD$_3$)$_2$CO solvent mixture [53]. The white data points are from Goodwin et al.'s original publication, and were also measured in a D$_2$O:(CD$_3$)$_2$CO mixed solvent (Fig. 9).
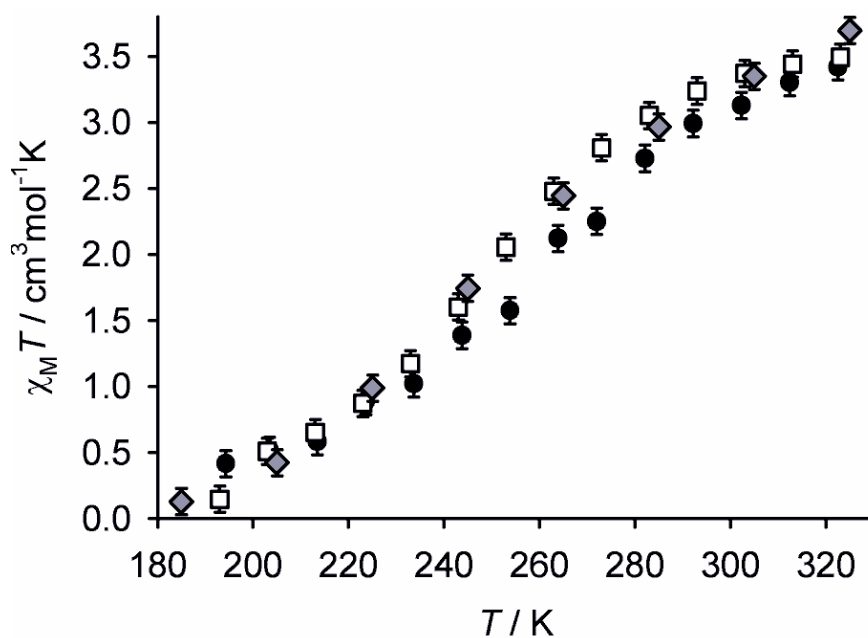
Fig. 11. Variable temperature magnetic susceptibility data for [Fe(1-bpp)$_2$][BF$_4$]$_2$ (♦) [22], [Fe(3-bpp)$_2$][BF$_4$]$_2$ (□) [46] and [Fe(1,3-bpp)$_2$][BF$_4$]$_2$ (●) in {CD$_3$}$_2$CO. Thermodynamic parameters from these equilibria are listed in Table 1.
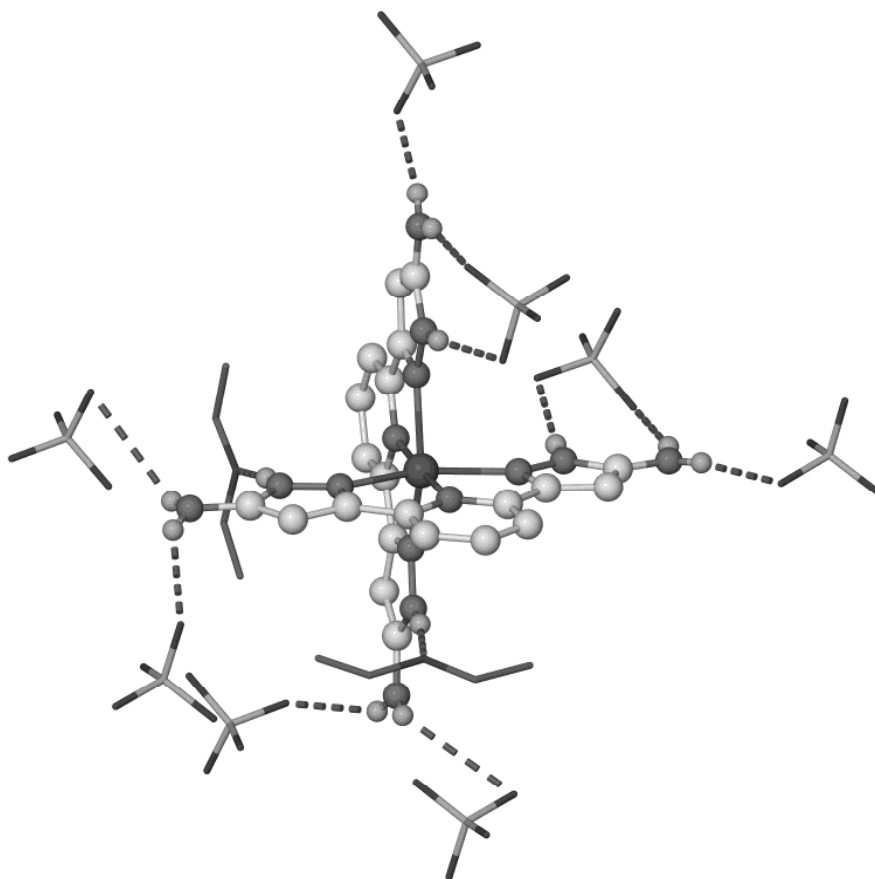
Fig. 12. Crystal structure of $[Fe(L^1)_2][ClO_4]_2 \cdot 2(C_2H_5)_2O \cdot CH_3NO_2$, showing the hydrogen bonding between the complex dication and the perchlorate anions and diethyl ether molecules (which are de-emphasised for clarity). The cations and anions are respectively eight-connected and four-connected nodes in a distorted **flu** network topology [60].
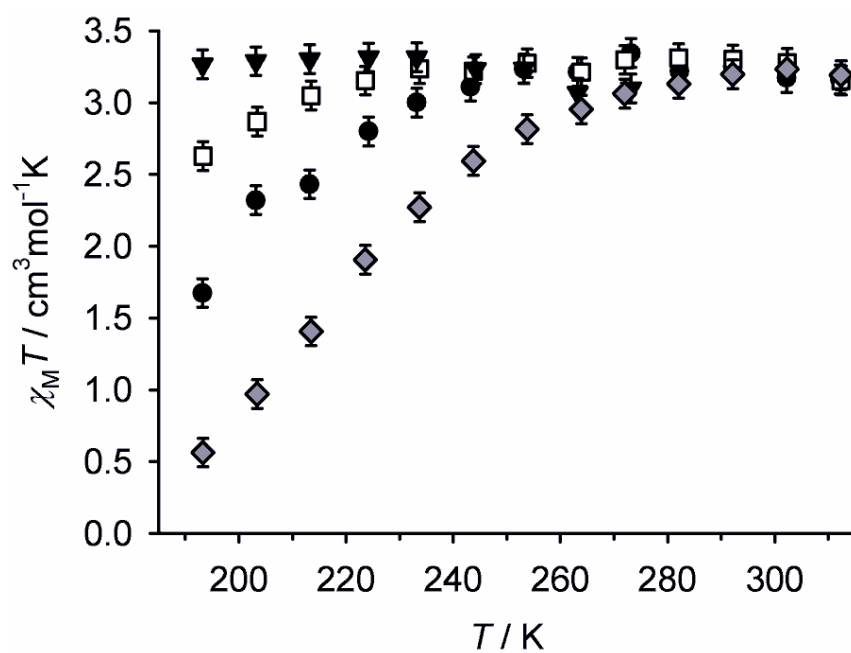
Fig. 13. Variable temperature magnetic susceptibility data for $[Fe(L^1)_2][ClO_4]_2$ (●), $[Fe(L^2tBu)_2][BF_4]_2$ (▼), $[Fe(L^3tBu)_2][BF_4]_2$ (□) and $[Fe(L^4Me)_2][BF_4]_2$ (♦) in $\{CD_3\}_2CO$.